Poster: X60: A Programmable Testbed for Wideband 60 GHz WLANs with Phased Arrays

Swetank Kumar Saha[1*], Yasaman Ghasempour[2*], Muhammad Kumail Haider[2*], Tariq Siddiqui[1],
Paulo De Melo[1], Neerad Somanchi[1], Luke Zakrajsek[1], Arjun Singh[1], Owen Torres[1],
Daniel Uvaydov[1], Josep Miquel Jornet[1], Edward Knightly[2], Dimitrios Koutsonikolas[1],
Dimitris Pados[1], Zhi Sun[1]

[1]University at Buffalo, SUNY, Buffalo NY, USA, [2]Rice University, Houston TX, USA
{swetankk,tariqsid,paulodem,neeradso,lukezakr,asingh29,owentorr,danieluv,jmjornet,dimitrio,pados,zhisun}@buffalo.
edu,{ghasempour,kumail.haider,knightly}@rice.edu

ABSTRACT

We introduce X60, the first SDR-based testbed for 60 GHz WLANs, featuring fully programmable MAC/PHY/Network layers, multi-Gbps rates, and a user-configurable 12-element phased antenna array. These features provide us with an unprecedented opportunity to revisit the most important aspects of 60 GHz signal propagation and obtain new insights on performance expected from practical 60 GHz systems. X60's unique capabilities make it an ideal platform for experimentation and prototyping across layers.

1 INTRODUCTION

The IEEE 802.11ad standard, using 2.16 GHz wide channels in the unlicensed band centered around 60 GHz and directional transmissions, provides data rates of up to 6.7 Gbps in an indoor WLAN setting. Realizing high-speed directional links, however, comes with challenges, sparking off research for the design of efficient link adaptation techniques. Nonetheless, most available experimental platforms either offer very limited access to the PHY/MAC layers (commercial devices) or use narrow band transmissions (USRP/WARP combined with a 60 GHz frontend) coupled with horn antennas (e.g., [2, 5]) deviating significantly from 802.11ad's use of ultra-wide channels and phased array antennas. This leaves a vacuum for a testbed that can offer the best of both worlds: a realistic PHY *and* programmability of PHY/MAC layers.

This poster introduces **X60**, the first highly configurable software defined radio (SDR) 60 GHz testbed, featuring fully *programmable PHY, MAC, and Network* layers, ultra-wide channels, and phased arrays. Based on the National Instrument's (NI) millimeter-wave (mmWave) Transceiver System [3] and equipped with *user-configurable* 12-element phased array antennas from SiBeam, X60 nodes (Figure 1) enable communication over **2 GHz** wide channels using

Figure 1: Two X60 nodes, each attached to a SiBeam phased array module.

realistic Tx and Rx beams that can be steered in **real-time** and support multi-gigabit data rates.

X60 offers several advantages over existing mmWave experimental platforms. Unlike commercial 802.11ad devices, X60 with its SDR/FPGA based architecture allows access to and complete control over the PHY and MAC layers. This not only enables experimentation that can obtain a full view of the often complex interaction among multiple layers of the networking stack, but also allows for prototyping and testing of new techniques at multiple layers. In contrast to most existing SDR mmWave platforms, X60 provides high reconfigurability without limiting baseband bandwidth to a few hundred MHz, enabling us to study the impact of extra wide channels supported by 802.11ad. Further, X60's phased arrays generate beam patterns that are configurable and steerable in real time, overcoming a basic limitation of horn-antenna based platforms.

The only testbeds capable of wide-band transmission with phased array antennas are OpenMili [6] and the testbed in [1]. OpenMili supports a channel width of 1 GHz and uses 4-element phased-arrays, with two possible values for each element's weight. The testbed in [1] uses 8-element phased arrays but operates in the 24 GHz band. In contrast, X60 has antenna 12 elements, 4 discrete possible phase values per element, and supports a 2 GHz channel width, enabling higher rate and higher resolution experiments.

X60's design and capabilities, for the first time, provide an opportunity to re-examine the current understanding of the most important aspects of 60 GHz WLAN signal propagation and performance. To this end, we summarize in this poster the results from an extensive measurement campaign across four characteristic indoor environments in a typical academic building. Our measurements encompass a range of propagation scenarios (dominant LoS, non-LoS only, reflections from multiple obstacles, LoS propagation with side-lobes) and Tx and Rx orientations.

---

2 X60 TESTBED

In the following, we describe the different components of the testbed. All the modules are programmed using NI LabVIEW.

Baseband Tx/Rx. Each X60 node is based on the NI mmWave Transceiver System. All modules involved in the baseband signal generation are assembled inside a NI PXIe-1085 PXI Express chassis. Most of the inter-module signaling and data transfer happens over the chassis's high-speed backplane using FIFO queues or DMA. The Tx/Rx chains consist of one or more high-performance FPGAs which handle the majority of the transmit/receive operations including encoding/decoding and modulation/demodulation. The FPGA outputs feed into an ultra-wideband DAC/ADC module which generates/samples the baseband signal. In addition, the chassis holds a high-end controller (host machine) that generates the source bits for transmission and is the sink for the receive operation. It controls different Tx/Rx parameters (MCS, uplink/downlink, etc.) and logs system information for user-display and debugging.

PHY/MAC Structure. The current reference PHY implementation supports the following MCS: 1/5 BPSK, 1/4 QPSK, 1/2 QPSK, 3/4 QPSK, 1/2 16QAM, 3/4 16QAM, 7/8 16QAM, resulting in theoretical bit rates from 300 Mbps to 4.75 Gbps. Data transmission takes place in 10 *ms frames* which are divided into 100 *slots* of 100 *μs* each. Both the MCS and operation type (uplink/downlink/sync) can be configured on a *per-slot* basis. A slot is made up of 92 codewords, each of which has an attached CRC block.

Antenna Array and Beam Patterns. The SiBeam mmWave module, in the Tx path, takes as input the baseband signal (as differential I/Q), up-converts, and transmits over the air a 2 GHz wide waveform centered around one of the 802.11ad channel center-frequencies. The Tx power is 30 dBm EIRP at channel 2. The in-built phased array has 24 elements; 12 for Tx and 12 for Rx. The module connects to the baseband chassis over an additional dedicated control path that allows different phase values for the antenna elements through the use of codebooks. The phase of each antenna element can be set to one of four values: $0, \pi/2, \pi, 3\pi/2$.

SiBeam's reference codebook defines 25 such beams spaced roughly 5° apart (in their main lobe's direction). The beams cover a sector of 120° (in the azimuthal plane) centered around the antenna's broadside direction. We refer to the beams using index range -12 (-60°) to +12 (+60 °), with index 0 corresponding to the broadside beam. The 3 dB beamwidth for the beams ranges from 25 to 30 degrees for Tx and from 30 to 35 degrees for Rx.

We computed the idealized beam patterns using COMSOL Multiphysics. Figs. 2a-2d depict examples of 2D and 3D radiation patterns for select beam indices. These patterns highlight how, in contrast to beams generated by horn antennas, phased-array generated beams often have strong side-lobes. Moreover, as beams are steered away from the main lobe, patterns become more imperfect with even stronger side lobes and a considerably weaker main lobe. For instance, comparing beam index 3 (Fig. 2b) and 12 (Fig. 2c) shows how practical phased-arrays can have *non-uniform steerability* along different directions as opposed to mechanically rotated horn antenna beams. Surprisingly, beam indices equally apart from the broadside beam (e.g., +3 (Fig. 2b) and -3 (Fig. 2d) can have radiation patterns that are *not* necessarily mirror images of each other.

These particular characteristics of the beam patterns result both

out of the discretization of the individual antenna element phase weights and the particular geometry in which the elements are arranged in the 2D array. Nitsche et al. [4] also found the beam patterns of commercial WiGig devices to be imperfect with strong side lobes. Also, an inspection of the open source wil6210 driver targeting Qualcomm 802.11ad chipsets suggests 2 bits for phase control of the antenna elements, allowing for 4 possible values.

2.1 Enhancements for Measurements

We made the following modifications to the reference code to enable logging of all the required PHY/MAC parameters and to allow for more realistic measurements. **Automatic Gain Control (AGC):** We implemented an AGC block running on the host machine (every 100 ms) that adjusts the receiver's gain value based on the energy calculated from the raw I/Q samples to achieve an experimentally determined optimal target energy value that ensures best ADC operation. Through a separate set of experiments, we verified that our implementation is throughput optimal (as compared to exhaustive-search manual gain control) for different MCS and channel conditions. **Thin Control Channel:** We added an external legacy WiFi radio to all four nodes to implement a reliable control path. This allows us to implement certain features like Tx-Rx beam selection or MCS selection and to automate parts of our measurements with only few modifications to the existing code base, without the burden of maintaining tight timing requirements of the code running the mmWave channel. The scripts that implement this control path run on the host machine and communicate with the LabVIEW process via IPC over TCP to control parameters like MCS and beam index, and collect link metrics for further processing. **Instrumentation:** We instrumented the host side LabVIEW code base to log a range of PHY/MAC layer parameters. Given that the host is an active part of the Tx/Rx flow and needs to maintain strict timing guarantees, we selected different logging frequency for each parameter to minimize overhead. Some parameters (Signal Power Estimation, Noise Power Mean, Throughput, CRC pattern) are logged on a per-frame basis (every 10 ms), while others (RSSI, SNR, Carrier-to-Noise, Phase, Power Delay Profile) are logged at a lower frequency (every 40 ms).

3 MEASUREMENT STUDY

3.1 Methodology

Our measurement campaign is aimed at collecting key PHY and MAC layer parameters across multiple indoor environments. Four indoor measurement locations – a narrow corridor, a lab with cardboard partitions and metal cabinets, a conference room with various metallic/shiny surfaces, and a lobby with large glass panels as walls – are selected to characterize static 60 GHz channels, as well as emulate typical mobility patterns like translation and rotation.

At each location, we collect channel measurements in two steps: *(i) Beam Sweep:* This step encompasses channel estimation for all possible beam pairs in an exhaustive search. The transmitter and receiver co-ordinate their beam switching (over the control channel) to generate all 625 (25x25) beam-pair combinations. For each beam pair, 25 frames are transmitted at MCS 0 and SNR is logged for the channel estimation slot in each frame (every 40*ms*). *(ii) MCS sweep:* In this step, we select a small subset of (Tx,Rx) beam pairs
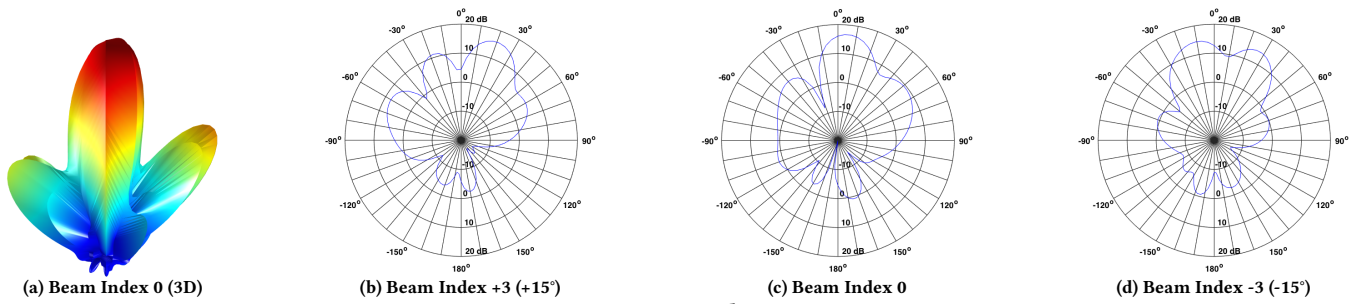
(a) Beam Index 0 (3D)   (b) Beam Index +3 (+15°)   (c) Beam Index 0   (d) Beam Index -3 (-15°)

Figure 2: Antenna array beam patterns.
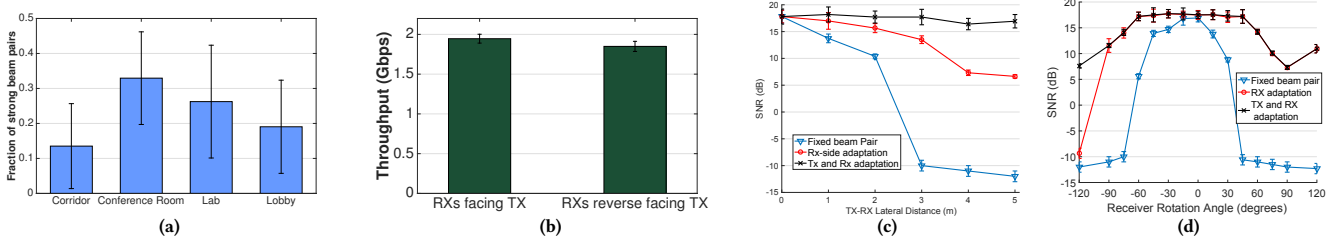

(a)   (b)   (c)   (d)

Figure 3: Experimental results: (a) Richness of strong beam pairs, (b) Throughput in LoS and NLoS positions, (c) Beam adaptation strategies for lateral translation, (d) Beam adaptation strategies for rotation.

for which we repeat measurements at all seven achievable MCS levels. We select the 3 strongest beam pairs out of all 625 beam pairs, based on average SNR computed during beam sweep in step (i). Further, to study the impact of selecting neighboring beams, we also include the immediate neighbors of the Rx beam in each of the three (Tx,Rx) pairs, for a total of nine (Tx,Rx) beam pairs. For each MCS, we log all channel parameters for 500 frame transmissions.

3.2 Experimental results

We summarize the most important findings in Figs. 3a-3d.

Richness of Strong Beam Pairs. Fig. 3a shows that the average (over all measurement positions) ratio of strong beam pairs (at least 10 dB SNR) is above 0.13 for all four environments, i.e., more than 80 beam pairs provide at least 1 Gbps of throughput. Hence, in contrast to the common belief, there are several beam pairs that are able to provide Gbps data rates for 60 GHz communication. The richness of strong beam pairs implies that beam adaptation algorithms might be able to avoid time-expensive exhaustive search through all beam combinations. Another implication is that interference between simultaneous transmissions may not be negligible in 60 GHz.

Performance of NLoS links. We consider the conference room since it has many reflectors such as whiteboard and TV screen and measure throughput in six positions. In three of them, there is a LoS path between the Tx and Rx; in the other three, the Tx and Rx face away from each other and can only communicate through a NLoS path (via reflections). Fig. 3b shows that the throughput is close to 1.9 Gbps in either case, with and without the LoS path, confirming that Gbps communication is feasible via reflections.

Beam Misalignment and Nodal Mobility. We analyze two typical mobility scenarios, lateral translation and rotation, in Figs. 3c, 3d, respectively. We consider three possible adaptation strategies: (i) fixed beams – we use beam pair (0,0), the default pair when the Tx and Rx face each other, (ii) Tx and Rx adaptation, and (iii) Rx-only adaptation. Fig. 3c plots the SNR with each strategy at 6 different

Rx positions in the lobby, emulating a path taken by a node as it moves perpendicularly to the Tx in steps of 1m. We observe that the gradient for the Rx-only adaptation curve is significantly better than the no-adaptation curve, and a link is sustained across all positions, indicating that a local search at the Rx, though sub-optimal, may be sufficient to maintain the link.

Fig. 3 plots the results for a scenario where the Rx was placed directly in front of Tx, 6.3 m apart, and the SiBeam antenna was rotated mechanically. Again, Rx-only adaptation achieves similar SNR as Tx-and-Rx adaptation, although the maximum achievable SNR diminishes for higher Rx angles on one side – a consequence of non-uniform angular spread of beam patterns and diminishing directivity gain of beam indices farther from the central beam, both limitations of practical phased array antennas. On the other hand, we found (graph omitted due to space limit) that, when the Tx and Rx are placed at a relative angle of 30°, Rx-only adaptation alone is not enough to sustain high SNR; this shows the importance of identifying different mobility scenarios for appropriate adaptation.

REFERENCES

[1] Omid Abari, Haitham Hassanieh, Michael Rodriguez, and Dina Katabi. 2016. Millimeter Wave Communications: from Point-to-Point Links to Agile Network Connections. In *Proc. of ACM HotNets*.

[2] Muhammad Kumail Haider and Edward W. Knightly. 2016. Mobility Resilience and Overhead Constrained Adaptation in Directional 60 GHz WLANs: Protocol Design and System Implementation. In *Proc. of ACM MobiHoc.*

[3] National Instruments. 2017. Introduction to the NI mmWave Transceiver System Hardware - National Instruments. http://www.ni.com/white-paper/53095/en/. (2017). (Accessed on 06/25/2017).

[4] Thomas Nitsche, Guillermo Bielsa, Irene Tejado, Adrian Loch, and Joerg Widmer. 2015. Boon and Bane of 60 GHz Networks: Practical Insights into Beamforming, Interference, and Frame Level Operation. In *Proc. of the 11th ACM CoNEXT.*

[5] Sanjib Sur, Vignesh Venkateswaran, Xinyu Zhang, and Parameswaran Ramanathan. 2015. 60 GHz Indoor Networking through Flexible Beams: A Link-Level Profiling. In *Proc. of ACM SIGMETRICS.*

[6] Jialiang Zhang, Xinyu Zhang, Pushkar Kulkarni, and Parameswaran Ramanathan. 2016. OpenMili: A 60 GHz Software Radio Platform With a Reconfigurable Phased-Array Antenna. In *Proceedings of the ACM MobiCom.*